Nonlinear Pre-yield Modal Properties of Timber Structures with Large-diameter Steel Dowel Connections

Citation for published version:
Reynolds, T, Harris, R & Chang, W-S 2014, 'Nonlinear Pre-yield Modal Properties of Timber Structures with Large-diameter Steel Dowel Connections', *Engineering Structures*, vol. 76, pp. 235-244.
https://doi.org/10.1016/j.engstruct.2014.07.010

Digital Object Identifier (DOI):
10.1016/j.engstruct.2014.07.010

Nonlinear pre-yield modal properties of timber structures with large-diameter steel dowel connections

This is the author's accepted version. For the published paper, please go to:

Thomas Reynolds[1], Richard Harris[2], Wen-Shao Chang[2]

[1](Corresponding Author) BRE Centre for Innovative Construction Materials, Department of Architecture and Civil Engineering, University of Bath, Claverton Down, BA2 7AY
tpsr20@bath.ac.uk

[2] BRE Centre for Innovative Construction Materials, Department of Architecture and Civil Engineering, University of Bath, Claverton Down, BA2 7AY

Abstract

In timber structures, the connections are generally flexible in comparison to the members they connect, and so contribute significantly to the dynamic properties of the structure. It is shown here that a widely-used form of connection, the dowel-type connection, exhibits nonlinear stiffness and energy dissipation, even at pre-yield loads, and that this nonlinearity affects the modal properties of structures with such connections. This study investigates that behaviour by modal analysis of a portal frame and a cantilever beam constructed from timber with steel dowel connections. The observed nonlinearity is explained qualitatively by considering the measured force-displacement response of individual connectors under cyclic load, which show a reduction in stiffness and an increase in energy dissipation with increasing amplitude of vibration. The structures were tested by modal analysis under slow sine sweep and pseudo-random excitation. Under pseudo-random excitation, a linear single degree-of-freedom curve fit was applied to estimate the equivalent linear modal properties for a given amplitude of applied force. Under slow sine sweep excitation, the frequency response function for the structures was observed to show features similar to a system with a cubic component of stiffness, and the modal properties of the structures were extracted using the equation of motion of such a system. The consequences for structural design and testing are that two key design parameters, natural frequency and damping, vary depending on the magnitude of vibration, and that parameters measured during in-situ testing of structures may be inaccurate for substantially different loads.

1.0 Introduction

The natural frequency and damping in a structure is often observed to vary as the amplitude of vibration varies. This variation is an important consideration in the design of structures for vibration, as it means that the stiffness and damping parameters used in design must correspond to the amplitude of vibration being considered. This has important consequences for in-situ testing of structures. The frequency and damping measured, for example, in modal tests at small amplitude may not be applicable to the larger-amplitude vibration in a severe wind event.

This study is concerned with the amplitude of vibration which a timber structure might experience as part of its everyday service life. Under such vibration, the forces in members and connections are well below their yield load, and the engineer must ensure that the vibration does not cause discomfort to occupants or users of the structure, or impede the proper use of the structure in any other way. Accurate dynamic properties are therefore required for design. It is shown that the nonlinear behaviour of connections in timber structures at these loads can lead to a variation in those dynamic properties.

There has been a great deal of research into the dynamic performance of timber structures with dowel-type connections under the forces and displacements associated with seismic loading, including experimental work and modelling of light timber frames with nailed sheathing [1-3], glued-laminated timber frames with bolts [4], cross-laminated structures connected by screws [5] and a complete light timber frame residential building [6].

Under loads representative of the seismic forces on a building, the nonlinearity of the force-displacement behaviour in connections is sufficient to justify detailed curve-fitting of the hysteretic loops, and their development under repeated cycles of load, such as carried out by Zhang et al. [7], whose model includes 13 parameters to represent pre- and post-yield behaviour, pinching, stiffness degradation and energy dissipation. Based on an understanding of the limitations of timber systems under seismic loads, special devices have then been added to such structures to improve their seismic response [8-10]. Modern lightweight timber structures may be susceptible to smaller-amplitude in-service vibration problems, for example under wind load [11, 12], and a more thorough understanding of that dynamic response is required for enhanced designs or special devices to be proposed.

Under smaller-amplitude vibration, the dynamic response of a structure can be reasonably represented by linear modal properties. A dynamic analysis of a 6-storey brick-clad timber frame building was carried out as part of the tests on the Building Research Establishment's Timber Frame 2000 project, presented by Ellis and Bougard [13]. Nonlinearity was evident even under the small-amplitude, pre-yield forces applied to this structure, and Ellis and Bougard noted the variation in natural frequency and damping in the structure with amplitude of excitation.

As modern engineered wood products are used to create more ambitious structures, the lack of knowledge of connection behaviour can make design of those structures for in-service vibration difficult, as noted by Utne [12] for the case of a multi-storey timber building, and there has already been an example of a timber bridge with unacceptable vibration attributed to movement in connections [14].

In contrast to seismic vibration, in-service vibration is often, though not exclusively, one-sided. That is to say, the mean component of the force on the structure is sufficiently large in comparison to the oscillating component that the force in the structure does not reverse, but maintains the same direction. Examples include footfall-induced vibration of a structure, in which the self-weight and imposed loads on the structure are far larger than the oscillating force imposed by footfall, and along-wind vibration, in which the mean wind load is large in comparison to the turbulent component. One-sided vibration is studied in this work.

Tests on individual dowel-type connections by Reynolds et al. [15] showed that, for cyclic loads with peak loads of 20% or 40% of the yield load, stiffness nonlinearity was evident, and stiffness was observed to reduce with an increase in amplitude of cyclic load.

This study uses loading representative of in-service vibration, such as might be imposed on a structure by wind or footfall, and investigates the variation in stiffness and damping resulting from nonlinearity in modes of vibration of two glulam frame structures. The nonlinearity is related qualitatively to the force-displacement behaviour observed in isolated connections. A simple single degree-of-freedom curve-fitting approach suitable for weakly non-linear modes is developed and applied to measure the variation in stiffness and damping in the structures as the amplitude of vibration is varied.

This work extends the field by relating the nonlinear vibration of timber structures under pre-yield loads to stiffness variation in their connections. It shows that, although they cannot describe it completely, Duffing's equations for a system with cubic stiffness can be used as an inverse modelling tool to extract information about that nonlinear vibration. It is also shown that, for a widely-used form of connection, modal properties, particularly damping, can vary dramatically with amplitude, and that variation is quantified for two structures in laboratory tests.

2.0 Behaviour of dowel-type connections

A series of tests was carried out investigating the response of a single dowel-type connector to cyclic loads, the results of which are presented by Reynolds et al. [15]. Some of the results from that paper are presented here with a different focus, to investigate how nonlinearity in the behaviour of connections may affect the dynamic response of the cantilever beams and frames tested in this study. Figure 1 shows the force-displacement diagram for two individual cycles of force, both having approximately the same mean force, on the same single-dowel connection specimen. The amplitude of the applied force differs between the two cycles by a factor of approximately 10. The gradient lines for calculation of the secant stiffness of each cycle are shown in the figure, and show that the secant stiffness is lower for the cycle with larger amplitude.

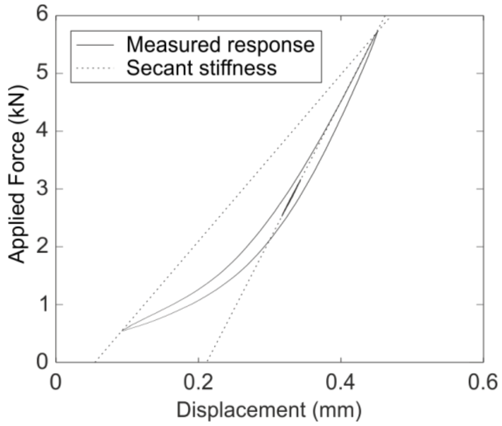

Figure 1 - Force-displacement plots for single cycles of force on a parallel-to-grain single-dowel connection specimen

The difference in energy dissipation between the two cycles in Figure 1 can also be seen, since the larger-amplitude cycle encloses a larger area.

The amplitude of the two cycles can be expressed as an R-ratio, which is the ratio of the highest to the lowest load in the cycle. Reynolds et al. [15] tested three specimens at R-ratios of 1.2 and 10 for specimens loaded in tension and compression, parallel and perpendicular to the grain. Here we compare the tests with a mean value of approximately 20% of the predicted yield load of the connection, to be of relevance to the frame and cantilever tests. The true mean load in the tests ranges between 16 and 22% of the predicted yield load of the connection. The variation of stiffness with amplitude is shown using the mean values for each of the three specimens tested in Figure 2, which shows that there is a consistent reduction in stiffness as the R-ratio is increased from 1.2 to 10.

The following qualitative characteristics were therefore noted in the single-dowel connection tests, which were expected to influence the behaviour of the complete connection and frame:

- a variation of stiffness with amplitude of applied force due to reduced stiffness at low load;

- a variation of energy dissipation with amplitude of applied force;

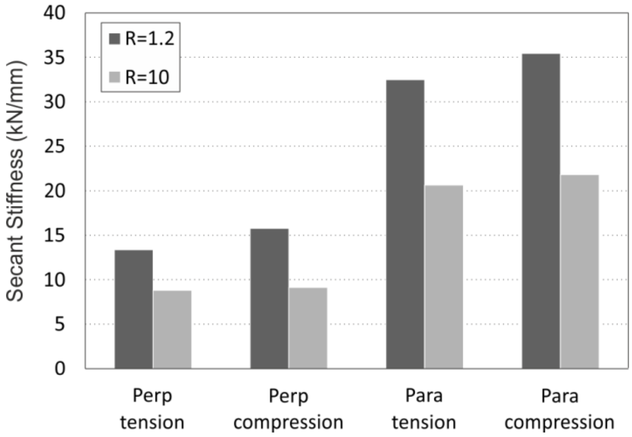

Figure 2 - Mean of secant stiffness for three specimens, varying *R*-ratio

3.0 Materials and methods

Two structural forms were tested, designed to illustrate the behaviour of connections as part of a complete structure. They were: 1.8 m long beams mounted as cantilevers (three specimens with two connection types each), and 1.8 m x 1.65 m vertically oriented portal frames (two specimens).

3.1 Materials

All the specimens were manufactured from a single batch of Norway spruce glued-laminated timber members. The members used in the frame tests were 185mm by 200mm, made up of five 40mm laminates and those used in the single-dowel connection tests were cut from those sections. The members in the portal frames were used as delivered, which meant that there were examples of knots being present near the holes through which the dowels passed. The mean density of the timber was estimated by weighing a 1.8m by 200mm by 185mm piece, giving a value of 458kg/m^3. Its moisture content was measured by electrical resistance after testing to be 11.3%. During testing, the ambient conditions were measured to range between 17.6 and 18.8°C and 55.0 and 60.3% relative humidity.

3.2 Geometry

The structures tested are shown schematically in Figure 3. The cantilever beam was supported by a moment connection to the laboratory strong wall and additional mass was imposed by the shaker (37kg) and, in the case of the four-dowel connection tests, a 30kg steel block at its end. The portal frame had moment connections at each node and was supported by moment connections on the strong wall with a total additional mass of 157kg imposed by four 30kg steel blocks and the shaker, placed at the lower moment resisting joint away from the wall. The portal frame was thus rotated from its normal configuration in a structure, which allowed the self-weight and additional mass to apply a load parallel to the line of the wall. Two portal frames and three cantilever beams were tested.

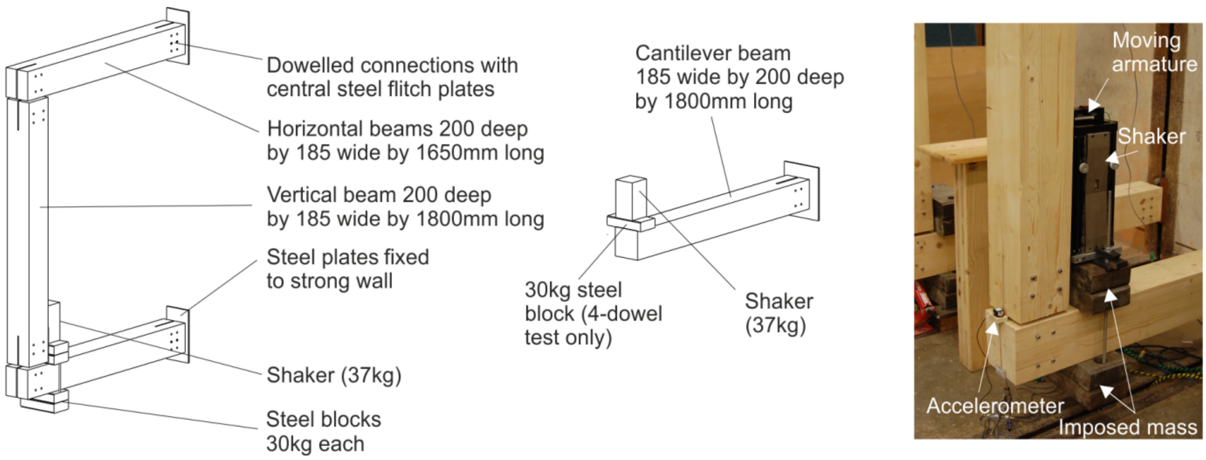

Figure 3 - Schematic test setup for modal analysis of frame structures and photograph of shaker mounted on frame

3.3 Connections

In all the tests, 12mm steel dowels were used, and passed through the timber member and a 6mm-thick steel plate inserted in a 7mm slot in the timber member. The holes in the timber were drilled using a 12mm-diameter auger drill bit, and the dowels were observed to fit tightly into the hole. As discussed further in [15], it is considered that nonlinearity in dowel embedment under cyclic load is primarily due to the nature of the contact surface between steel and timber, with any lack-of-fit between dowel and timber resulting mainly in additional initial displacement. In the cantilever beams and the supports of the frames, the steel plate was welded to a bracket fixed to the laboratory strong wall. Figure 4 shows the geometry of a generalized connection, along with reference numbers for each hole.

In the portal frame specimens, six-dowel connections were used at the support points and four-dowel connections were used at the nodes away from the wall, due to the lower load on the connections at those nodes. The three repetitions of both two- and four-dowel connections were formed by reusing the vertical member from the frame structures, and testing the connections at each end, with each connection tested first with four dowels, and then with two dowels. This would have led to a total of four connections being tested, but one of the connections was not tested due to damage which occurred while dismantling the frame specimen. The dowel arrangements in each connection, and the loads applied to each structure, are shown in Table 1.

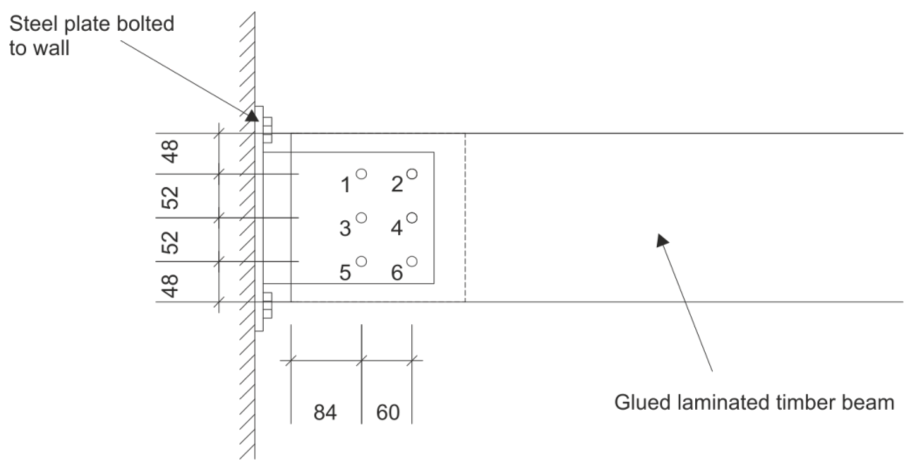

Figure 4 - Geometry of connections and numbering of holes (dimensions in millimetres)

Table 1 – Connections and loading in test specimens - see Figure 4 for dowel locations

Connection	Number of dowels	Dowel locations	Applied mass (kg)
Cantilevers A2, B2, C2	2	1,5	37 (Shaker only)
Cantilevers A4, B4, C4	4	1, 2, 5, 6	67 (Shaker + 30kg steel block)
Frames A and B - node	4	1, 2, 5, 6	157 (Shaker + 4×30kg steel blocks)
- support	6	1 to 6	

3.4 Loading, Excitation *and Instrumentation*

The dynamic properties of the frames were measured by carrying out modal analysis of the measured displacements and accelerations due to excitation by an electrodynamic shaker. The shaker applied a force to the structure through the inertia of an armature which moved along a single axis, driven by an inductive coil. Since the shaker was placed on the structure and otherwise unsupported, the variable force applied to the structure was generated by the inertia of the moving armature, and so was proportional to its acceleration. By attaching an accelerometer to the armature, the applied force could be calculated from the measured acceleration.

Two separate methods were used to dynamically excite each frame, each requiring a different analysis method. Both were forced vibration tests, exciting the structure at a single point. To preserve the simplicity of analysis in both cases, the excitation was applied at the same point as the imposed mass: at the end of the cantilever and at the bottom right angle joint of the frame. This also meant that the mass of the shaker, significant at 37kg, formed part of the imposed mass. By carrying out a stiffness-matrix analysis of the portal frame, and allowing for the flexibility in the connections, the static loads imposed on the structure from self-weight, the weight of the shaker and that of the steel blocks were shown to load the highest loaded connector to 20% of the predicted yield load, according to Eurocade 5 [16]. In the cantilever beams, the load was 30% of the predicted yield load for the two-dowel connections and 20% for the four-dowel connections.

The excitation methods were:

- a slow sine sweep, in which a sinusoidal force, gradually increasing in frequency, was applied by the shaker and the rate of increase of frequency was sufficiently slow that the steady-state response at each frequency had time to develop; and
- pseudo-random excitation, in which a signal containing a known range of frequency components, with random phase was generated and used to drive the shaker.

In the cantilever beam tests, the slow sine sweep and pseudo-random excitation covered a range of frequencies from 4 to 14Hz. In the frame tests, that range was from 6 to 14Hz.

Before dynamic testing, the structures (both cantilevers and portal frames) were assembled, instrumented and propped at the point where the mass was to be placed. The prop was set at a height that made the horizontal members level, as measured with a spirit level. The prop was then removed, and the displacement monitored to allow the anticipated transient processes to occur: looseness in the connections to be taken up; surface irregularities at the dowel-timber interface to crush as far as possible; and the initial viscoelastic behaviour in the connections to occur. This static loading was continued until the change in displacement due to creep in a minute was less than 0.1% of the total deflection. For the first loading of a connection, this took of the order of 10 hours. The dynamic tests were then carried out.

The relationship between the measured acceleration of the armature and the force applied to the supporting structure, by the shaker, was calibrated using a load cell. The shaker was mounted on the load cell, and the armature caused to oscillate at a frequency of 8Hz, representative of the natural frequency of the cantilever and frame structures. The measured plots of force and acceleration were then compared and used to estimate the constant of proportionality between the two. The result was that the constant was estimated as 23N/g, equivalent to a mass of approximately 2.3kg.

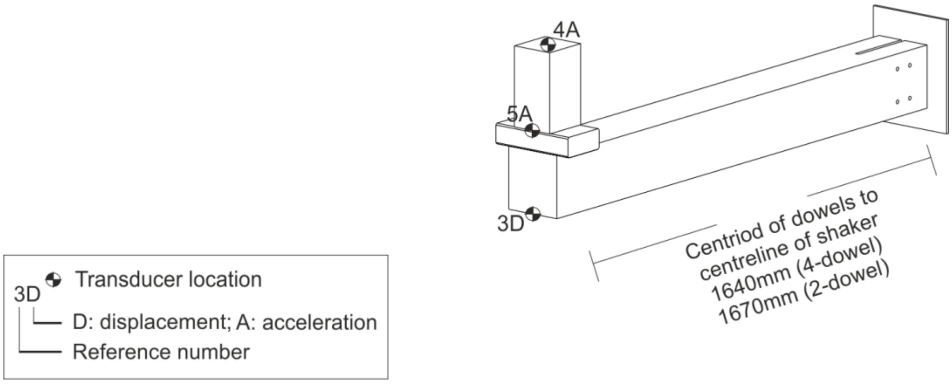

Figure 5 - Transducer locations on cantilever beam specimens

The structures were instrumented so that both displacement and acceleration of various points of the structure could be measured. The location of the sensors for the cantilevers and frames are shown in Figure 5 and Figure 6 respectively. Given the time history of the force applied to the structure, calculated from the acceleration of the shaker armature, and the time history of displacement and acceleration from these sensors, the receptance and accelerance could be directly calculated.

The input force spectrum could therefore be obtained from the measured acceleration of the shaker armature. The amplitude of the force applied in each test was expressed as a proportion of the yield load calculated according to Eurocode 5 [16], and the nominal value is shown in the test matrix in Table 2. The loads applied to the structure in reality differed slightly from these nominal loads, and the measured amplitude of applied loads is used for the analysis in Section 4.0.

The response was measured from the accelerometers and displacement transducers around the structure. The concentration of mass in each structure, and the fact that the excitation was applied along a single axis, meant that the response of each was dominated by a single mode of vibration. The purpose of the modal analysis was to identify the natural frequency and modal damping, as well as the presence of any nonlinearity, in that single mode.

Table 2 - Test matrix

Specimen	Test Number	Loading Type	Nominal RMS Amplitude (% of yield)
Cantilever A2	1	Slow sine sweep	0.75%
	2	Slow sine sweep	1.5%
	3	Pseudo-random	0.25%
	4	Pseudo-random	0.5%
Cantilever B2	1	Slow sine sweep	0.75%
	2	Slow sine sweep	1.5%
	3	Pseudo-random	0.25%
	4	Pseudo-random	0.5%
Cantilever C2	1	Slow sine sweep	0.75%
	2	Slow sine sweep	1.5%
	3	Pseudo-random	0.25%
	4	Pseudo-random	0.5%
Cantilever A4	1	Slow sine sweep	0.375%
	2	Slow sine sweep	0.75%
	3	Pseudo-random	0.125%
	4	Pseudo-random	0.25%
Cantilever B4	1	Slow sine sweep	0.375%
	2	Slow sine sweep	0.75%
	3	Pseudo-random	0.125%
	4	Pseudo-random	0.25%
Cantilever C4	1	Slow sine sweep	0.375%
	2	Slow sine sweep	0.75%
	3	Pseudo-random	0.125%
	4	Pseudo-random	0.25%
Frame A	1	Slow sine sweep	0.125%
	2	Slow sine sweep	0.25%
	3	Slow sine sweep	0.375%
	4	Slow sine sweep	0.5%
	5	Pseudo-random	0.125%
	6	Pseudo-random	0.25%
	7	Pseudo-random	0.375%
	8	Pseudo-random	0.5%
Frame B	1	Slow sine sweep	0.125%
	2	Slow sine sweep	0.25%
	3	Slow sine sweep	0.375%
	4	Slow sine sweep	0.5%
	5	Pseudo-random	0.125%
	6	Pseudo-random	0.25%
	7	Pseudo-random	0.375%
	8	Pseudo-random	0.5%

For the pseudo-random tests, the precision of the measured transfer function depended on the sampling rate and the length of the measured time-histories of displacement and force. Pilot tests showed that a test of 100s duration sampled at 200Hz provided a sufficiently well-defined transfer function, and these were used on the pseudo-random vibration tests on the cantilever joints and frames.

In the slow sine sweep tests, a sampling rate of 200Hz was again used. The duration of the test was chosen so that the rate of sweep was slow enough for the full resonant response to develop at each frequency of applied force.

The natural frequency and damping of the mode in consideration influence the time taken for the system to reach its steady-state response at resonance, and so influence the rate at which the frequency should be increased in a slow sine sweep test. ISO 7626 [17] gives an equation for the appropriate rate of sweep for modal analysis for a model with a given natural frequency and damping (1). n is frequency in Hertz, n_n is the natural frequency of the mode in question, γ is the equivalent viscous damping ratio and t is time.

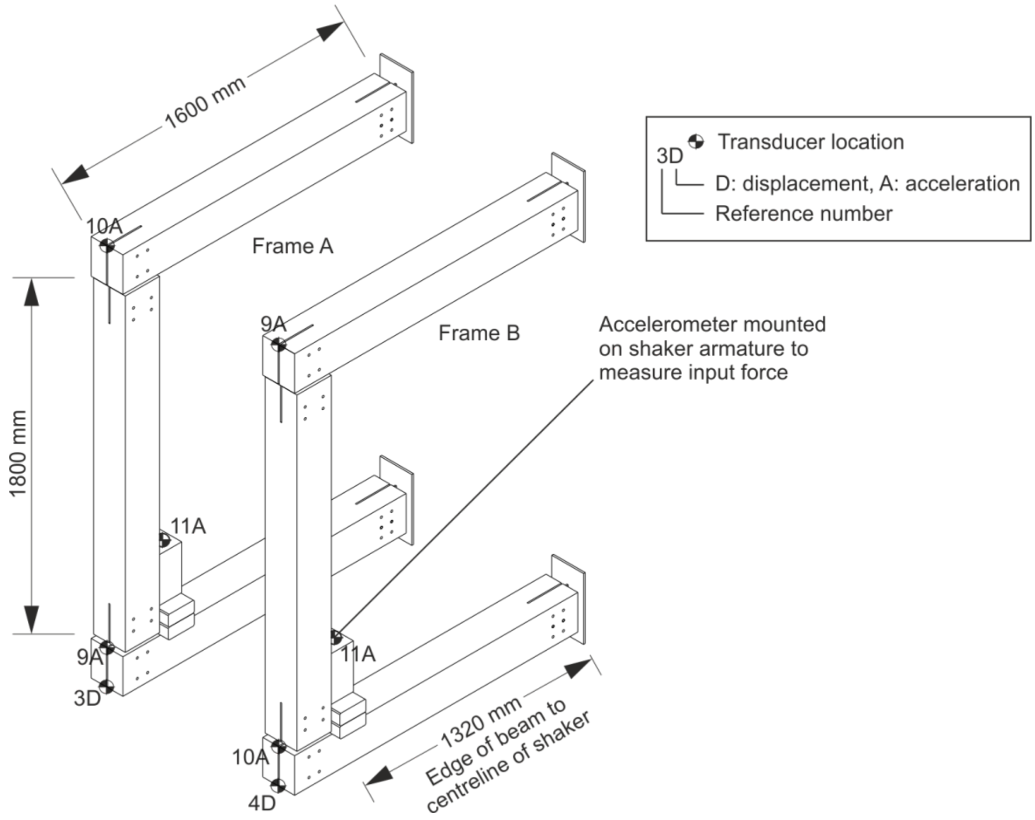

Figure 6 - Transducer locations on frame specimens

$$\left.\frac{dn}{dt}\right|_{max} = 216\frac{n_n^2}{\gamma^2} \ldots (1)$$

The natural frequency of the system was estimated based on pilot tests and a conservatively low estimate of damping, 1.5%, was used to determine the sweep rate of 1.5Hz/min for use in the tests.

Once the tests had been conducted, the accelerance was plotted from the measured acceleration, by converting the time histories of force and acceleration to their frequency-domain spectra using a discrete Fourier transform, MATLAB's built-in *fft* function, and then dividing acceleration by force at each frequency. The accelerance could be transformed to receptance by a frequency-domain transformation.

For the case of pseudo-random excitation, a more accurate measurement of the accelerance H_a can be made by using the relationship between it, the autocorrelation of the input force P_{ff} and the cross correlation between force and acceleration P_{fa} [18], as given by (2). A similar relationship exists for receptance.

$$H_a = \frac{P_{fa}}{P_{ff}} \dots (2)$$

The amplitude of the applied cyclic load was varied to observe the effect on stiffness and energy dissipation, and on the form of the receptance function. The tests were designed to measure the steady-state stiffness and damping at each amplitude of applied load, the transient effects being eliminated by applying a static load for a period before the test, and restarting the tests if any significant change in the modal properties or displacement was noted during the application of the oscillating load.

3.5 Modal Identification

The use of correlation functions to estimate the transfer function for pseudo-random excitation implies an assumption that the modal properties are constant throughout the test. As a result, the transfer function which is generated is a linearization of the true behaviour and, as long as the true behaviour is sufficiently close to linear, linear modal identification techniques can be applied. In this case, a least-squares curve fit was carried out by linearizing the error function between the measured and modelled accelerance, and then solving to find the complex natural frequency and the residue to minimize that error function [19].

In contrast to the tests with pseudo-random excitation, the accelerance plots for slow sine sweep excitation showed the presence of nonlinearity in the system. Specifically, the asymmetry in the receptance spectrum suggested a weakly nonlinear system with softening. A mathematical representation of softening behaviour is given by Duffing [20], who carried out an extensive study into the equation given in (3), which describes the oscillation of a system with undamped natural frequency ω_n and viscous damping ratio γ, under a harmonic force f. The linear restoring force in Duffing's oscillator is generated by the natural frequency squared ω_n^2, equal to the linear stiffness per unit mass k/m, multiplied by the displacement x. There is also a component of the restoring force proportional to x^3, with constant of proportionality μ. This will be referred to as the cubic stiffness. Duffing's equation is therefore identical to the equation of motion for a single degree-of-freedom dynamic system, but with an additional cubic stiffness component in the restoring force.

$$\ddot{x} + 2\gamma\omega_n\dot{x} + \omega_n^2 x + \mu x^3 = f \dots (3)$$

The cubic stiffness term μ represents a system whose secant stiffness changes with amplitude. A positive value of μ represents a 'hardening' system, whose stiffness increases with amplitude, and a negative value represents a 'softening' system whose stiffness decreases. Figure 7 shows the receptance for the Duffing oscillator with three different magnitudes of the cubic component of stiffness. In this example, for illustration, ω_n is 31.4rad/s, γ is 0.02 and μ is zero ('Linear'), -4×10^{6}N/mm^3/kg ('Softening 1'), and -8×10^{6}N/mm^3/kg ('Softening 2'). It can be seen that the peak magnitude of receptance moves to a lower frequency, and both the magnitude and phase plots become asymmetrical. Once a certain degree of nonlinearity is achieved, as in the line labelled Softening 2, the receptance can be seen to jump between two values for a very small change in frequency. This discontinuity occurs at a frequency of a little over 9.5 Hz in Figure 7.

It should be noted that the softening system, despite having a lower stiffness than the linear one, can exhibit a lower magnitude of response than the linear system with the same damping due to a less clear resonance, as in the case of the line labelled 'Softening 2'.

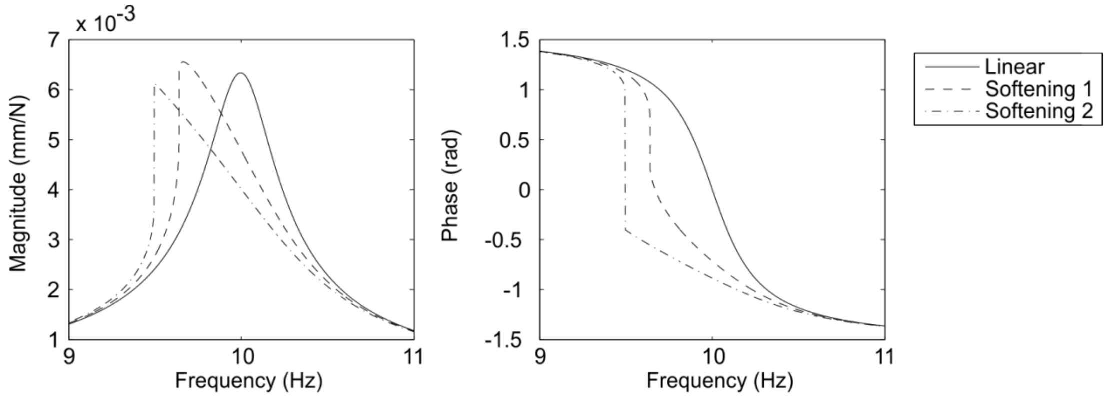

Figure 7 - Magnitude and phase of receptance for systems with varying cubic stiffness component: the cubic stiffness, *μ in (3)*, is zero in the linear case, and 'Softening 2' has a cubic stiffness double that of 'Softening 1'

Duffing's oscillator therefore exhibits a variation of secant stiffness with amplitude, defined by μ. For amplitude of oscillation X, the secant stiffness is equal to the linear stiffness plus μX^2. The real variation of stiffness in a structure will not, in general, follow this relationship, so the cubic stiffness model was not expected to fit the measured receptance of the cantilever and portal frame structures over a large range of amplitudes.

Since the vibration was dominated by a single mode, four parameters define the acceleration curve: the modal mass, the linear natural frequency, the damping and the cubic stiffness component. The modal mass was taken from an eigenvalue analysis of the estimated stiffness and mass matrices of the system. The remaining three parameters were then fitted using a multidimensional unconstrained nonlinear minimization algorithm through Matlab's ® *fminsearch* function, using the sum of squares of the difference between the measured and fitted curves as the function for minimization.

Figure 8 shows curves fitted to the measured receptance of a slow sine sweep test on Frame A using different ranges of points. It can be seen that if too wide a range of points is used for the curve fitting, the cubic function does not fit the behaviour at high and low amplitudes well, resulting in a poor representation of the measured receptance, as in the right hand plot in Figure 8, where all receptance measurements higher than a quarter of the peak value were used to fit the curve.

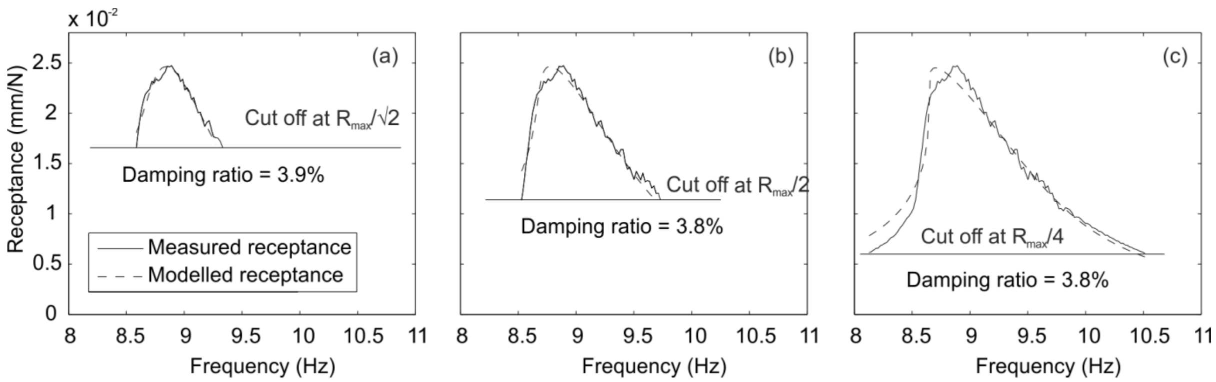

Figure 8 - Curve fitting the cubic stiffness model to the measured receptance for Frame A using a) all values greater than the peak value divided by √2, b) all values greater than the peak value divided by 2 and c) all values greater than the peak value divided by 4

The left hand plot in Figure 8 shows a much closer fit to the measured receptance over the smaller range of values. This suggests that the parameters of the cubic function are not constant, but vary with amplitude of vibration, that is, the damping varies with amplitude and the variation of stiffness does not follow the cubic stiffness model perfectly. A representative damping ratio was extracted for each specimen by fitting the cubic function to all values of receptance greater than the peak value divided by two, equivalent to the central plot in Figure 8. It was considered that, in this manner, sufficient points would be fitted to reasonably represent the measurements, while restricting the range of amplitudes, so that the cubic function provided a reasonable fit.

4.0 Results *and Discussion*

An example of the result of the single degree-of-freedom curve-fitting process, ***in this case for the cantilever beam B4,*** is shown in Figure 9. It can be seen that the measured accelerance deviates substantially at some points from the fitted curve for a linear single degree-of-freedom system. It is considered that this is likely to be due to the nonlinearity in the system, rather than simply measurement noise, since, as the results of the slow sine sweep tests suggest, the stiffness and damping vary with amplitude, and so would be expected to vary continuously throughout the duration of the pseudo-random excitation. The linear approximation is therefore considered to represent an average of the behaviour throughout the test.

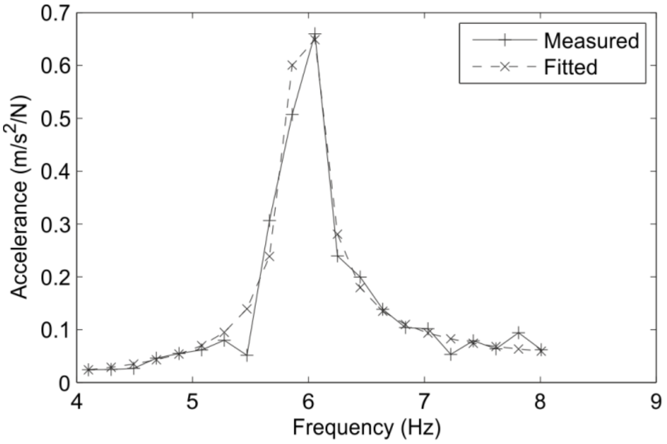

Figure 9 - Single degree-of-freedom curve fit for cantilever beam specimen B4 with a four-dowel connection

Figure 10 shows the magnitude and phase of receptance for the same cantilever beam specimen. It can be seen that, in contrast to the linearized spectrum in Figure 9, the accelerance plot is asymmetrical, and shows a sharp increase in accelerance at approximately 5.5Hz. This is considered to be equivalent to the discontinuity observed in the cubic stiffness model and shown in Figure 7. The slight oscillation in the receptance spectrum, in both magnitude and phase, either side of the discontinuity is considered to be due to the finite rate of sweep which was used, which can not perfectly represent the discontinuity.

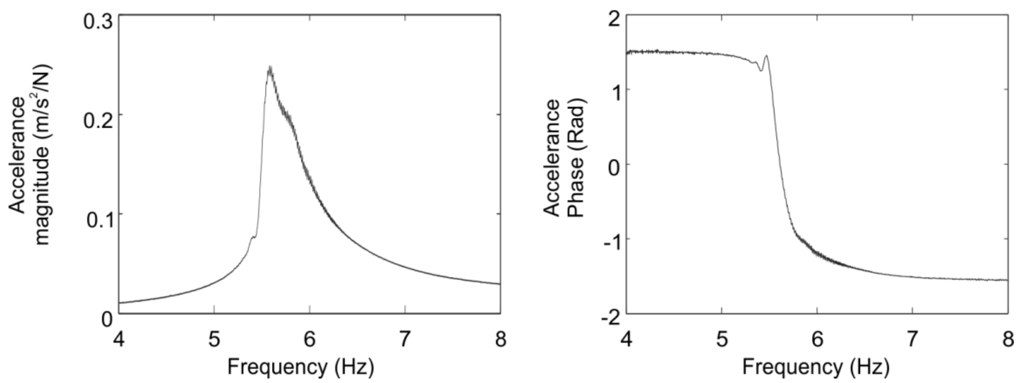

Figure 10 - Accelerance for slow sine sweep test on cantilever beam specimen B4 with a four-dowel connection

The measured modal properties for all the cantilever beam specimens are shown in Figure 11. The amplitude of the excitation force is expressed as the root mean square (RMS) value, to aid comparison between the pseudo-random and slow sine sweep tests. In the slow sine sweep tests, the amplitude of the sine wave is constant, and given by the RMS value multiplied by √2, and the sweep is sufficiently slow as to allow resonance to fully develop at each frequency. In the tests with pseudo-random excitation, the amplitude varies continuously, and so resonance is not allowed to fully develop in the same way, although the response is dominated by that at the resonant frequency. Slow sine sweep and pseudo-random tests with the same RMS value of force would not, therefore, be expected to give the same modal properties. The RMS value is, however, considered to be a reasonable measure with which to compare the two forms of excitation. The RMS force is expressed as a percentage of the load which would be expected to cause yield of the connection, according to the Eurocode 5 [16] design method. There was a slight variation in the RMS force applied to the different specimens due to the effect of the vibration on the force generated by the shaker, so Figure 11 gives the range of RMS force for the three repetitions.

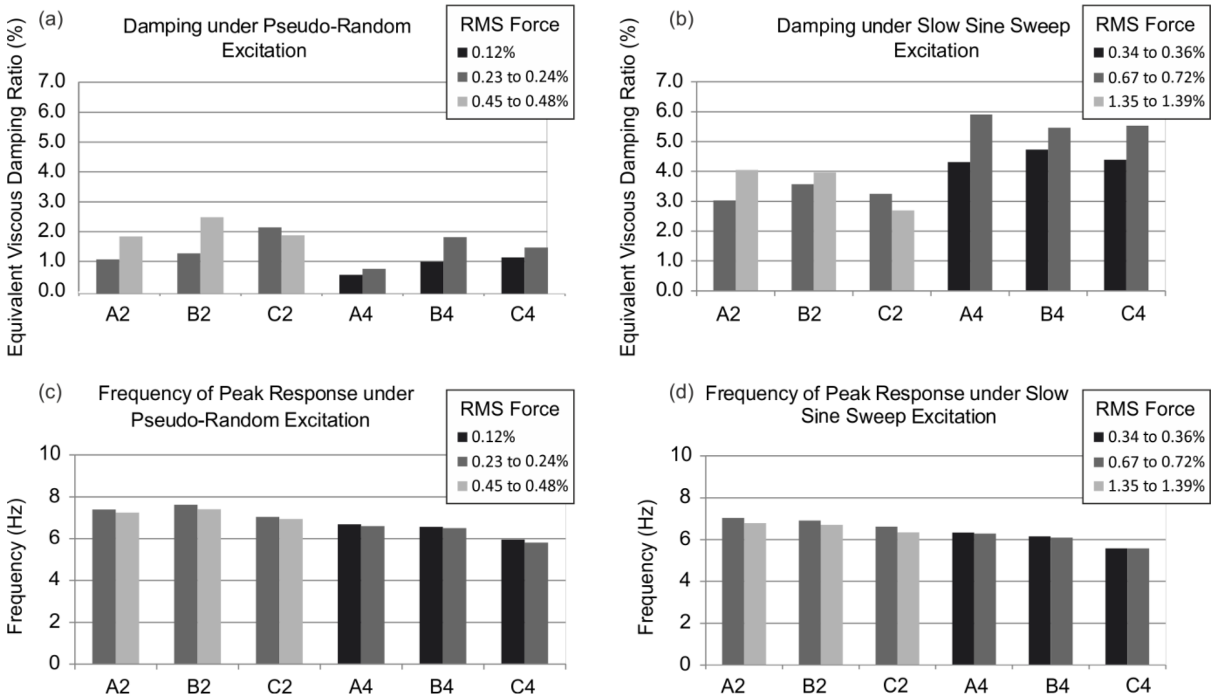

Figure 11 - Modal properties for cantilever specimens with two- and four-dowel connections at two amplitudes of excitation, with the root mean square (RMS) force expressed as a percentage of the *yield* load. ***The damping is shown in (a) for pseudo-random excitation and in (b) for slow sine sweep. The frequency of the peak response is in (c) for pseudo-random, and (d) for slow sine sweep excitation.***

The effect of the reduced stiffness at low load, observed in connection tests, can be seen in the tests on the cantilever specimens. The nonlinear force-displacement behaviour in the connections means that the frequency of the peak response varies with the amplitude of the applied force, as shown in (c) and (d) in Figure 11. The softening behaviour in the connections results in a reduction of stiffness, and therefore a reduction in the frequency of the peak response, as the amplitude of the applied force is increased. This reduction occurs consistently across all the tests, with the exception of test C4 under slow sine sweep excitation, in (d), where the reduction was zero. In all the tests, the reduction in frequency due to the increase of the applied cyclic load ranges from zero to 4.1%.

More dramatic, but more scattered, changes were observed in the damping, which ranged from a 17% reduction, to a 77% increase, as shown in (a) and (b) in Figure 11. Only one specimen exhibited a reduction in damping, but for that specimen***, C2***, a reduction was observed under both slow sine sweep and pseudo-random excitation. It is considered that this may be because the nonlinear behaviour in the connection alone caused a reduction in the amplitude of vibration. This can be seen to be theoretically possible as shown in Figure 7, and the reduced amplitude of vibration may have led to a reduced damping.

The lower excitation forces under pseudo-random excitation lead to generally lower damping than in the slow sine sweep tests, which can be seen by comparing (a) and (b) in Figure 11. Under the higher-amplitude response to the slow sine sweep excitation in (b) the damping is higher in the four-dowel connections than the two-dowel connections.

Figure 12 shows the results for the frame specimens. Each frame was tested at three amplitudes of applied load under each form of excitation. The consistent reduction in the frequency of the peak response with amplitude can again be seen, in (c) and (d), and there is a strong effect on damping, though not in every case. Each frame exhibits higher damping and a lower frequency of the peak response under slow sine sweep excitation than pseudo-random excitation, as shown in (a) and (b), and both effects are considered to be due to the higher amplitude of movement under slow sine sweep excitation, since the full resonant response is allowed to develop.

It is again seen, in Figure 12, to be not always the case that damping increases with amplitude of excitation, since Frame A under pseudo-random excitation, shown in (a), appears to reach an approximate plateau of damping above approximately 0.2% RMS force. Higher damping ratios are, however, recorded in that frame under slow sine sweep excitation. It is considered that the increase in damping with the increase in amplitude is due to limiting friction being overcome in gradually increasing areas of contact between moving parts of the structure, such as between the dowel and the timber around it, or the steel plate and the dowel. As a result, it is thought to be reasonable that plateaus in damping such as for Frame A in (a) in Figure 12 would occur when more movement is required to overcome limiting friction in the next area. (b) shows that damping does continue to increase with the increased amplitude of movement in that specimen, after the plateau shown in (a), since the full resonance developed under slows sine sweep excitation gives a greater amplitude of movement.

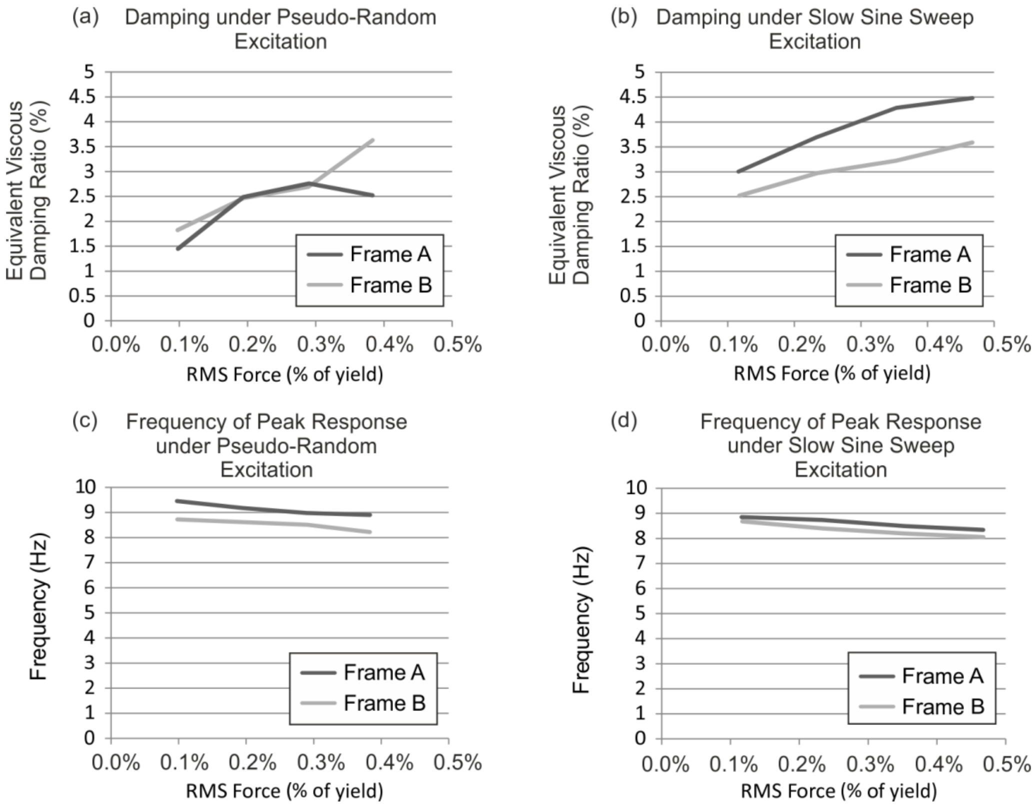

Figure 12 - Modal properties for frame specimens plotted against the root mean square (RMS) of the input force, expressed as a percentage of the load required to cause *yield* in the most loaded connection. The variation of damping is shown in (a) for pseudo-random excitation, and in (b) for slow sine sweep. The frequency of peak response is illustrated in (c) for pseudo random, and (d) for slow sine sweep excitation.

5.0 Conclusion

Nonlinear force-displacement behaviour in connections at low loads has been observed to lead to a reduction in secant stiffness with an increase in amplitude of one-sided cyclic load. As a result, timber structures with dowel-type connections exhibit modal properties which vary with amplitude under the one-sided cyclic loads typical of in-service vibration induced by wind or footfall. The experimental results given by this study show that there is an influence of amplitude of applied force on the natural frequency and damping in timber structures with dowelled connections under pre-yield loads.

The most pronounced influence is on damping, though the influence of amplitude on damping was not consistent in all tests, with some showing similar, or reduced damping over certain ranges of amplitude.

The measured receptance function was shown to exhibit similar features to a system with a cubic component of stiffness, in that the receptance function was asymmetrical, and in some cases exhibited a discontinuity below the frequency of the peak response. By using a nonlinear minimization algorithm, the equation of a system with cubic stiffness was fitted to the measured response, which allowed the damping ratio to be estimated.

Dowelled and dowel-type connections are widely used in timber structures, and the use of engineered wood products to create long-span and multi-storey timber structures means that in-service vibration is becoming an important design criterion. This work shows that the effect of the connections leads to such structures potentially exhibiting the characteristics of a softening system, with the consequences of varying natural frequency and damping with amplitude, and a fundamentally different form of frequency response.

6.0 References

[1] Polensek, A. & Schimel, B. D. Dynamic properties of light-frame wood subsystems. *Journal of Structural Engineering,* 117(4): 1079-1095, 1991, DOI: 10.1061/(ASCE)0733-9445(1991)117:4(1079).

[2] Filiatrault, A., Isoda, H. & Folz, B. Hysteretic damping of wood framed buildings. *Engineering Structures,* 25(4): 461-471, 2003, DOI: 10.1016/s0141-0296(02)00187-6.

[3] Folz, B. & Filiatrault, A. Cyclic analysis of wood shear walls. *Journal of Structural Engineering,* 127(4): 433-441, 2001, DOI: 10.1061/(asce)0733-9445(2001)127:4(433).

[4] Heiduschke, A. Analysis of wood-composite laminated frames under dynamic loads - Analytical models and model validation. Part I: Connection model. *Progress in Structural Engineering and Materials,* 8(3): 103-110, 2006.

[5] Ceccotti, A., Sandhaas, C., Okabe, M., Yasumura, M., Minowa, C. & Kawai, N. SOFIE project – 3D shaking table test on a seven-storey full-scale cross-laminated timber building. *Earthquake Engineering & Structural Dynamics*, 42(13): 2003-2021, 2013, 10.1002/eqe.2309.

[6] Filiatrault, A., Christovasilis, I. P., Wanitkorkul, A. & Lindt, J. W. V. D. Experimental seismic response of a full-scale light-frame wood building. *Journal of Structural Engineering,* 136(3): 246-254, 2010.

[7] Zhang, H., Foliente, G. C., Yang, Y. & Ma, F. Parameter identification of inelastic structures under dynamic loads. *Earthquake Engineering & Structural Dynamics,* 31(5): 1113-1130, 2002, DOI: 10.1002/eqe.151.

[8] Filiatrault, A. Analytical predictions of the seismic response of friction damped timber shear walls. *Earthquake Engineering & Structural Dynamics,* 19(2): 259-273, 1990, DOI: 10.1002/eqe.4290190209.

[9] Loo, W. Y., Kun, C., Quenneville, P. & Chouw, N. Experimental testing of a rocking timber shear wall with slip-friction connectors. *Earthquake Engineering & Structural Dynamics* 2014, DOI: 10.1002/eqe.2413.

[10] Kasal, B., Pospisil, S., Jirovsky, I., Heiduschke, A., Drdacky, M. & Haller, P. Seismic performance of laminated timber frames with fiber-reinforced joints. *Earthquake Engineering & Structural Dynamics,* 33(5): 633-646, 2004, DOI: 10.1002/eqe.368.

[11] Heiduschke, A. Performance and drift levels of tall timber frame buildings under seismic and wind loads. *Structural Engineering International,* 18(2): 186-191, 2008.

[12] Utne, I. 2013. *Numerical Models for Dynamic Properties of a 14 Storey Timber Building.* Master of Engineering, Norwegian University of Science and Technology.

[13] Ellis, B. R. & Bougard, A. J. Dynamic testing and stiffness evaluation of a six-storey timber framed building during construction. *Engineering Structures,* 23(10): 1232-1242, 2001, DOI: 10.1016/s0141-0296(01)00033-5.

[14] Rönnquist, A., Wollebæk, L. & Bell, K.: Dynamic behavior and analysis of a slender timber footbridge. In: *World Conference on Timber Engineering*, Portland, Oregon. 2006.

[15] Reynolds, T., Harris, R. & Chang, W.-S. Stiffness of dowel-type timber connections under pre-yield oscillating loads. *Engineering Structures,* 65(0): 21-29, 2014, DOI: 10.1016/j.engstruct.2014.01.024.

[16] BS EN 1995-1-1:2004+A1:2008, *Eurocode 5 Design of timber structures Part 1-1: General — Common rules and rules for buildings*, BSI, 2009.

[17] ISO 7626-2:1990, *Method for experimental determination of mechanical mobility - Part 2: Measurements using single-point translation excitation with an attached vibration exciter* ISO, 1990.

[18] Ewins, D. J.: Modal testing: theory and practice. Research Studies Press Ltd. Baldock, Hertfordshire, England, 1986.

[19] He, J. & Fu, Z.-F.: Modal Analysis. Butterworth-Heinemann Oxford, 2001.

[20] Duffing, G.: Erzwungene Schwingungen bei veränderlicher Eigenfrequenz und ihre technische bedeutung. F. Vieweg & Sohn Braunschweig, 1918.